

# Journal of Biomedical Optics

[SPIEDigitalLibrary.org/jbo](http://SPIEDigitalLibrary.org/jbo)

## **Vasodilation by *in vivo* activation of astrocyte endfeet via two-photon calcium uncaging as a strategy to prevent brain ischemia**

Yuanxin Chen  
James Mancuso  
Zhen Zhao  
Xuping Li  
Jie Cheng  
Gustavo Roman  
Stephen T. C. Wong

# Vasodilation by *in vivo* activation of astrocyte endfeet via two-photon calcium uncaging as a strategy to prevent brain ischemia

Yuanxin Chen,<sup>a</sup> James Mancuso,<sup>a</sup> Zhen Zhao,<sup>a,b</sup> Xuping Li,<sup>a</sup> Jie Cheng,<sup>a</sup> Gustavo Roman,<sup>c</sup> and Stephen T. C. Wong<sup>a,\*</sup>

<sup>a</sup>Weill Cornell Medical College, Houston Methodist Research Institute, \Systems Medicine and Bioengineering Department, TT and WF Chao Center for BRAIN, Houston, Texas 77030

<sup>b</sup>Southeast University, Zhongda Hospital, Medical School, Department of Radiology, Jiangsu Key Laboratory of Molecular and Functional Imaging, Nanjing 210009, China

<sup>c</sup>Weill Cornell Medical College, Houston Methodist Hospital, Nantz National Alzheimer Center, Houston, Texas 77030

**Abstract.** Decreased cerebral blood flow causes brain ischemia and plays an important role in the pathophysiology of many neurodegenerative diseases, including Alzheimer's disease and vascular dementia. In this study, we photomodulated astrocytes in the live animal by a combination of two-photon calcium uncaging in the astrocyte endfoot and *in vivo* imaging of neurovasculature and astrocytes by intravital two-photon microscopy after labeling with cell type specific fluorescent dyes. Our study demonstrates that photomodulation at the endfoot of a single astrocyte led to a 25% increase in the diameter of a neighboring arteriole, which is a crucial factor regulating cerebral microcirculation in downstream capillaries. Two-photon uncaging in the astrocyte soma or endfoot near veins does not show the same effect on microcirculation. These experimental results suggest that infrared photomodulation on astrocyte endfeet may be a strategy to increase cerebral local microcirculation and thus prevent brain ischemia. © The Authors. Published by SPIE under a Creative Commons Attribution 3.0 Unported License. Distribution or reproduction of this work in whole or in part requires full attribution of the original publication, including its DOI. [DOI: [10.1117/1.JBO.18.12.126012](https://doi.org/10.1117/1.JBO.18.12.126012)]

Keywords: astrocytes–vasculature; infrared femtosecond laser; cerebral microcirculation; intravital two-photon microscopy; calcium uncaging.

Paper 130675LR received Sep. 16, 2013; revised manuscript received Nov. 4, 2013; accepted for publication Nov. 5, 2013; published online Dec. 16, 2013.

## 1 Introduction

Decrease of cerebral blood flow (CBF) reduces oxygen and substrate for brain metabolism and gives rise to brain ischemia, which is involved with pathological synaptic dysfunction,<sup>1</sup> circulatory deficiencies, neuronal loss, and memory deficits.<sup>2,3</sup> The progression of cerebral amyloid angiopathy affects vasodilation and promotes neurovascular units to release vasoconstrictive substances to suppress CBF and amplify cellular stress, which ultimately contribute to cognitive defects.<sup>4</sup> In addition, epidemiological, pharmacotherapy, and clinical imaging studies indicate that vascular changes play an important role in the reduction of CBF present in the early stages of Alzheimer's disease (AD) pathogenesis.<sup>5,6</sup>

Astrocytes, electrically nonexcitable cells, are clearly involved in the response and progression of neurodegeneration; they have a protective role in the initial response to neurodegeneration, but later may exert a negative effect through inflammation.<sup>7</sup> Astrocytes are the key component coupling the neurovascular unit and supply energy and oxygen for neuronal metabolism by converting glucose to lactate.<sup>3,8–10</sup> In addition, astrocytes have long been hypothesized to be involved in blood–brain material exchange<sup>11</sup> and cerebrovascular regulation through direct interaction between the astrocyte endfoot and arterioles that play a key role in arteriole vasodilation and

increase of local blood flow in the capillary.<sup>12–14</sup> Though certain optical imaging approaches, such as two-photon intravital microscopy, dynamic light scattering, and spectrally enhanced microscopy, have been used to image the vascular network and measure blood microcirculation,<sup>15,16</sup> their focus has been on observation and diagnosis, but not intervention, of CBF or brain ischemia. The *in vivo* photomodulation technique reported in this study can not only serve an observational and diagnostic function, but also provide a real-time, interactive strategy to increase local CBF of the live animal under observation and thus, serve as a powerful tool to delineate and understand the circuitry and dysfunction of neurovasculature.

Recently, astrocyte activation has been proposed as a potential means to increase local CBF<sup>13</sup> and as a novel therapeutic target for neurodegeneration, such as AD.<sup>7</sup> It is well known that astrocyte activation plays a key role in protection from neurodegeneration and causes arteriole vasodilation to provide more energy for brain metabolism.<sup>17</sup> Specific activation of the astrocyte endfoot may be the most direct method to control this interaction. Calcium uncaging, optogenetic activation, electromechanical stimulation, and pharmacological application have been deployed to activate astrocytes.<sup>13,18,19</sup> Due to the limitation of light scattering and diffusion, single-photon calcium uncaging with ultraviolet (UV) light cannot provide the high spatial resolution to specifically target the astrocyte endfoot around the arterioles, particularly those more than 30  $\mu\text{m}$  below the cortical surface. To this end, the optogenetic approach can be applied to specific targets and to activate astrocytes for

\*Address all correspondence to: Stephen T. C. Wong, E-mail: [STWong@tmhs.org](mailto:STWong@tmhs.org)

chronic treatments with high spatiotemporal resolution.<sup>18</sup> However, the introduction of external opsin proteins into the astrocyte membrane through viral expression limits its application in human patients. Mechanical and electrical stimulation would also need the invasive insertion of electrodes into the brain to activate astrocytes with uncertain side effects.

Here we report a new strategy of photomodulation that applies infrared (IR) two-photon laser irradiation to specifically target the endfeet of astrocytes around arterioles and performs calcium uncaging in the deep brain with high spatial resolution to increase local CBF in downstream capillaries *in vivo*, with the goal to prevent brain starvation and ischemic neuronal damage.

## 2 Materials and Methods

### 2.1 Animal Preparation

Three-month-old male C57BL/6J mice were anesthetized by the inhalation of isoflurane (4% for induction; 1.5 to 2% for surgery, and 1 to 1.5% for imaging). After anesthesia, dexamethasone and buprenorphine were subcutaneously administered, and 20 to 30  $\mu$ l 1% lidocaine solution was injected into the scalp to reduce pain. Fifteen minutes after the removal of the scalp, a high-speed microdrill was used to make a 3-mm-diameter craniotomy over the primary somatosensory cortex (centered 1 to 2 mm posterior to the bregma and 2 to 3 mm from the midline) under the dissecting microscope and a custom-made metal plate was glued on the skull with dental acrylic cement. After injecting the mixture of dyes into the cortex, 1% agarose gel and a 5 mm cover slip were added onto the exposed cortex to protect the exposed cortex and to reduce movement artifacts caused by respiration. Body temperature was monitored by a rectal probe and maintained at 37.1°C by a heating blanket (Homeothermic blanket systems, Harvard Apparatus, Holliston, Massachusetts). Experiments were performed only if the physiological variables remained within normal limits. All experiments were performed under the Institutional Animal Care and Use Committees approval of Houston Methodist Research Institute.

### 2.2 Dye Injection

Pluronic F-127 (20% dissolved in dimethyl sulfoxide) was used to dissolve (acetyloxy)methyl ester (AM) ester dyes, and these dyes were diluted to the specific concentration [Oregon Green<sup>®</sup> 488 BAPTA-1 AM (OGB-1 AM), 1 mM; *o*-nitrophenyl 6,9-dioxo-3,12-diazatetradecanedioic acid, 3,12-bis(carboxymethyl)-4-(2-nitrophenyl) (NP-EGTA), 200 mM] using saline solution. Under the two-photon microscope, the mixture of OGB-1, Sulforhodamine 101 (SR 101), and NP-EGTA-AM was administered via an IM-300 microinjector (Narishige, Japan) into the somatosensory cortex (200  $\mu$ m below the surface); 10 psi air pressure was used to perform dye injection for 90 s.<sup>20,21</sup> After washing and removing the dyes or blood left on the surface, we poured saline containing 1% agarose onto the exposed cortex and mounted a cover slip (5 mm diameter). Thirty to forty-five minutes after the recovery of the mouse from surgery, imaging was performed under intravital two-photon microscopy. Five minutes before imaging, fluorescein isothiocyanate-dextran (FITC-dextran, 70,000 kDa, 12.5 m/kg) was systemically administered into the tail vein to visualize cerebral vasculature and blood flow.

### 2.3 In Vivo Two-Photon Imaging and Calcium Uncaging

The upright laser scanning microscope (BX61WI, Olympus) was attached to a Ti:sapphire femtosecond pulsed laser system (80 MHz repetition rate, <100 fs pulse width, Spectra Physics, Santa Clara, California) and the software (Fluoview 1000) was used for two-photon fluorescence imaging. 5 $\times$  air, 25 $\times$  water-immersion [NA, 1.05; working distance (WD), 2 mm, Olympus], and 40 $\times$  water-immersion objectives (NA 0.80, WD; 3.3 mm, Olympus) were selectively chosen for fluorescence imaging *in vivo*. To excite OGB-1 and SR 101 simultaneously, 800-nm irradiation was used, and emission light was detected with 515/50 and 605/55 filters, respectively. In addition, we visualized pial arteries and veins under widefield fluorescence and identified penetrating arteries or collecting veins (10 to 35  $\mu$ m diameter) by following the direction of flow from the pial surface.<sup>22</sup> Capillaries were identified by their diameter ( $\sim$ 5  $\mu$ m). The average laser power for imaging was <30 mW. Arterioles, capillaries, and veins were discriminated by vessel diameter and blood flow direction. Series stacks of 512  $\times$  512  $\mu$ m<sup>2</sup> images (step-size: 1  $\mu$ m) were acquired from the cortical surface to depths below  $\sim$ 300  $\mu$ m by vertically translating the objective of the two-photon intravital microscopy system.

For calcium uncaging, the IR optical system (Ti:sapphire femtosecond pulse laser) was applied for photolysis; 800-nm IR laser (the output of average power 40 to 60 mW, <100 fs pulse width, 80 MHz repetition, physics spectra) was chosen to pinpoint target astrocyte endfeet surrounding arterioles and astrocyte soma to cause calcium uncaging. We started with low laser power and steadily increased the power until calcium uncaging could be visualized. The output power for the laser stimulation was controlled from 15 to 60 mW and stimulation duration was 0.5 to 1 ms.

### 2.4 Data Analysis

In all the experiments, we analyzed and processed image data using software Image J (NIH) and MATLAB<sup>®</sup>. The intensity of fluorescence signals was defined as  $\Delta F = (F_1 - F_0)/F_0$ , where  $F_1$  and  $F_0$  were fluorescence intensity in the astrocytes and background signal at the same time point; fluorescence intensity of the images before the stimulation was averaged as baseline intensity and relative calcium change was calculated based on  $\Delta F/B = (F - B)/B$ , where  $F$  and  $B$  were fluorescence intensity in the astrocytes at any given time point and baseline intensity, respectively.

The diameter of arteriole lumen was determined based on the distance between paired points across the arteriole directly adjacent to an identified endfoot and arteriole diameter of the images before stimulation averaged as baseline diameter. So the relative change of arterioles was defined as  $\Delta D = (D_1 - D_0)/D_0$ , where  $D_1$  was arteriole lumen diameter at any given time point and  $D_0$  was baseline diameter, respectively.

## 3 Results

Brain ischemia results from the deficiency of blood flow.<sup>1</sup> To characterize the role of astrocytes in the regulation of cerebral blood flow, a tunable, finely controllable Ti:sapphire femtosecond laser was employed to perform the visualization of astrocyte-vasculature interactions over the exposed somatosensory cortex. To determine the imaging area of interest, a small vessel

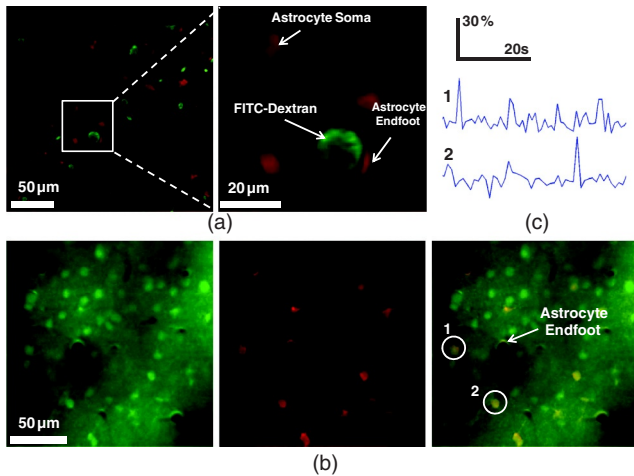


**Fig. 1** Imaging of cerebral vasculature, calcium signal, and astrocytes. (a) Image of the interaction of cerebral vasculature and astrocytes; to the right, the magnification of the white square; red, SR101 labeled astrocytes, green, FITC-dextran labeled cerebral vasculature. (b) Images of calcium signal and astrocytes; left, calcium signal imaging; middle, SR101 labeled astrocytes; and right, overlap left and middle. (c) Calcium transient for cells 1 and 2 in (b).

area was chosen to avoid the interference of large vessel shadows according to the maximum intensity projection of our imaging stack. In order to enhance image contrast, we introduced two specific dyes (FITC-dextran, SR 101) to visualize cerebral vasculature [Fig. 1(a): green] and astrocytes [Fig. 1(a): red], respectively. In addition, astrocyte endfeet, the processes ensheathed around the arteriole [Fig. 1(a), right], can be visualized while vessels, including arteriole, capillary, and vein, can be discriminated based on blood flow direction and diameter size of vessel lumen.

Astrocytes release glial transmitters in response to calcium influx specifically in the endfoot. In order to monitor physiological dynamics and signal transmission in astrocytes, the calcium signal indicator (OGB-1 AM) was administered into the somatosensory cortex 150 to 200  $\mu\text{m}$  below the surface to monitor the change of the calcium signal [Fig. 1(b), left]. Due to nonspecific labeling of OGB-1, the astrocyte-specific dye SR 101 was introduced to ensure the accuracy of astrocyte visualization [Fig. 1(b), middle and right]. Also, spontaneous calcium transients were regarded as the index to ensure the targeted astrocyte's viability [Fig. 1(c)].

UV light calcium uncaging of astrocyte endfeet around the arteriole gives rise to an increase of lumen diameter of the arteriole in the healthy animal model.<sup>12,13</sup> However, this method has the limitations of lower spatial resolution and lower stimulation depth due to light scattering. In order to finely control astrocyte activity and arteriole lumen diameter, we introduced the stimulation of IR two-photon irradiation to perform calcium uncaging in astrocytes and to measure the effect on arteriole vasodilation [Fig. 2(a)]. The mixture of NP-EGTA AM, OGB-1 AM, and SR 101 was administered into the area of interest in the exposed somatosensory cortex, and we used the same optical path as the two-photon imaging system to perform laser stimulation to perform calcium uncaging in astrocytes [Fig. 2(a)]. IR two-photon laser was used to specifically stimulate astrocyte somas, disregarding the vessel; the laser power was adjusted from low to high until the calcium signal increase was detected. We found

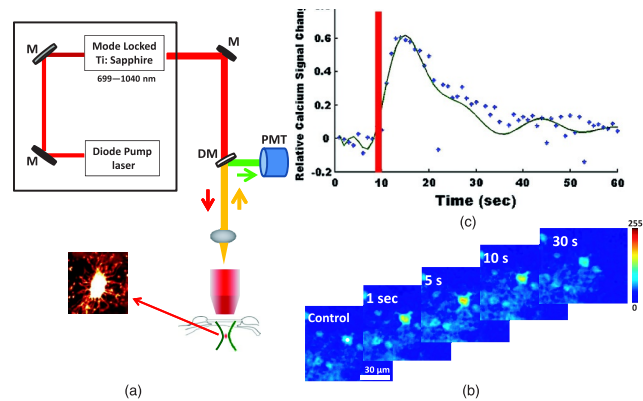


**Fig. 2** A schematic illustration of calcium imaging and calcium uncaging system. (a) Schematic illustration of calcium uncaging system using IR two-photon laser irradiation. (b) Time-series images of calcium uncaging exposed to the stimulation of IR two-photon laser irradiation. (c) Time-course tracings show that photostimulation causes a rapid increase of calcium signal and arterial vasodilation in the experiment shown in (b).

that the calcium signal increases after laser stimulation and reaches its maximum 10 s later [Figs. 2(b) and 2(c)].

We investigated whether or not two-photon astrocyte activation gives rise to vasodilation in the arteriole *in vivo*. In our study, calcium signal in the endfoot increased rapidly and reached its maximum 10 s later; in addition, it lasted 60 to 80 s after laser stimulation on the endfoot. The increase of arteriole lumen followed the increase of the calcium signal and reached its maximum 20 s later with a duration of  $\sim 60$  s. As shown in Figs. 3(a) and 3(b), the diameter of arteriole lumen increased  $\sim 25\%$  [Figs. 3(a) and 3(b)]. Zhao et al.<sup>23</sup> suggested

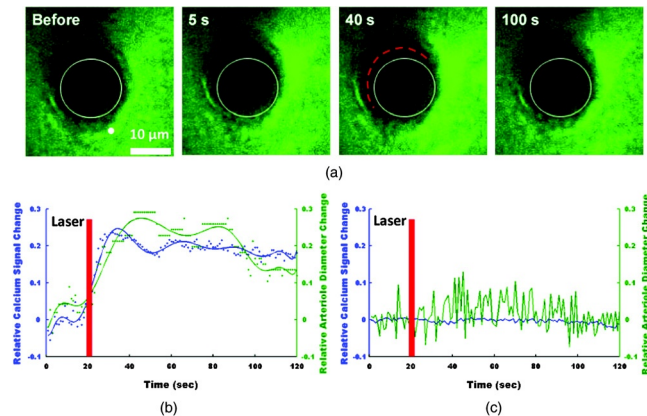


**Fig. 3** Calcium uncaging in astrocyte endfoot causes vasodilation in the arteriole. (a) Time-series images of arterioles diameter and calcium uncaging exposed to the stimulation of IR two-photon laser irradiation. Calcium uncaging triggered a rapid increase of  $\text{Ca}^{2+}$  in astrocyte endfoot and arterial vasodilation. White spot indicates the position of photostimulation. (b) Time-course tracings show that photostimulation causes a rapid increase of calcium signal and arterial vasodilation in the experiment shown in (a). (c) Photostimulation has no effect on both  $\text{Ca}^{2+}$  increase in astrocyte endfoot and arteriole vasodilation without NP-EGTA AM injection in the somatosensory cortex. White circle represents arteriole diameter, red dash curve represents the border of arterioles after photoactivation, blue curve indicates relative calcium signal change, and green curve indicates relative arterioles diameter change.

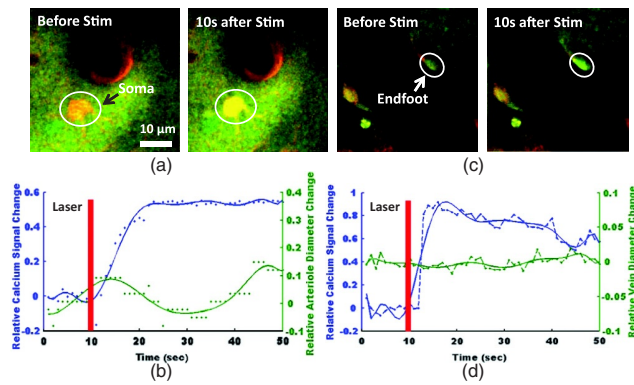


**Fig. 4** Calcium uncaging in astrocyte soma and endfoot does not cause vasodilation in arteriole and vein, respectively. (a) The relative change of arteriole diameter and calcium signal in astrocytes soma before and 10 s after calcium uncaging in an astrocyte soma. (b) Time-course tracings of  $\text{Ca}^{2+}$  change in astrocyte soma and arteriole diameter change. (c) The relative change of vein diameter and calcium signal in astrocytes endfoot around the vein before and 10 s after calcium uncaging in an astrocyte endfoot. (d) Time-course tracings of  $\text{Ca}^{2+}$  change in astrocyte endfoot around the vein and the diameter change of vein's lumen. Note: color intensity in (a) and (c) represents calcium signal intensity in astrocytes.

that a femtosecond pulse laser could target astrocyte membranes and increase calcium in cultured astrocytes; this raised the question of whether the vasodilation was not directly caused by calcium uncaging, but by laser stimulation on the astrocyte membrane. Thus, we injected the mixture of OGB-1 and SR 101 into the cortex, excluding NP-EGTA AM, and repeated the same experiment, but the same effect did not occur [Fig. 3(c)]; this result indicates that arteriole vasodilation was caused by calcium uncaging in the astrocyte endfoot.

Due to the large size of the astrocyte soma, specific targeting of the soma was more readily done than on the astrocyte processes. Therefore, we addressed another question: could we specifically stimulate the soma, instead of the endfoot, to increase the lumen diameter of arteriole? When calcium uncaging in the astrocyte soma occurred under the stimulation of IR two-photon laser, the calcium signal increased and reached the maximum 10 s after laser stimulation, but vasodilation in the neighboring arteriole did not occur [Figs. 4(a) and 4(b)]. In addition, astrocyte endfeet ensheathed around the vessel, including the arteriole, the capillary, and the vein, so under microscopy, blood flow direction is a good objective criteria to discriminate the arteriole and vein, but this introduced some difficulties in finding a stimulation site to perform calcium uncaging. To investigate whether the endfoot around the arteriole is the only potential stimulation site for vasodilation, we tested whether calcium uncaging on the astrocyte endfoot around the vein increased the lumen diameter of the vein; the results, however, showed that calcium increases in the endfoot around the vein had no effect on the vasodilation [Figs. 4(c) and 4(d)]. Hence, we concluded that IR two-photon laser irradiation could be employed to target astrocyte endfeet in order to perform calcium uncaging studies. Moreover, only calcium uncaging in astrocyte endfeet triggered by femtosecond laser caused the increase of arteriole lumen and subsequently increased the local blood flow in downstream capillaries.

#### 4 Conclusions and Discussions

Recent studies<sup>24,25</sup> demonstrate that decreased cerebral microcirculation, resulting in a deficiency of energy supply, causes

neuronal dysfunction and chronic brain ischemia and has a crucial role in the progression of a variety of neurological diseases, including AD. Our experimental results show that activation of individual astrocyte endfeet around the arteriole increases lumen diameter of the arteriole by 25%, which should subsequently increase local CBF to supply energy for brain metabolism. Furthermore, because gap junctions transmit signals between adjoined astrocytes,<sup>26–28</sup> the effect of vasodilation may spread to relatively distant areas and contribute to the same effect. These findings suggest that improving CBF for brain metabolism would be an effective and potentially therapeutic strategy to prevent or treat neurovascular or neurodegenerative diseases.

Though UV light has been used to perform calcium uncaging in astrocyte endfeet and increase local blood flow in downstream capillaries,<sup>12,13</sup> the stimulation site cannot be narrowed down to a subcellular structure due to light scattering and diffraction. Because of the small focal volume and reduced light scattering for IR two-photon excitation, our imaging technique can resolve this problem by targeting stimulation volumes down to femtoliters and can be used to address specific targets in astrocytes, as well as study and modulate physiology dynamics of the astrocytes in deep brain regions.

In addition, some calcium-caging reagents have been developed for use under IR femtosecond laser stimulation:<sup>17</sup> DM-nitrophen and azid-1 can not only be excited by UV irradiation, but also can have a maximum excitation at the specific long wavelength stimulation between 700 and 800 nm. Under 700-nm femtosecond laser irradiation and high-numerical-aperture objective, azid-1 can be photolyzed with a 10- $\mu\text{s}$  pulse train of 7 mW average power.<sup>17</sup> However, during the two-photon imaging process, the lower energy output of IR femtosecond pulse laser will make the occurrence of chemically irreversible calcium uncaging possible, which will interfere with calcium imaging. Compared with these calcium caging reagents, NP-EGTA AM is not as sensitive to femtosecond IR laser uncaging and needs relatively high energy to cause photolysis, which can reduce the possibility of unnecessary calcium uncaging during two-photon imaging.

Label-free stimulation by IR two-photon lasers has been introduced to nondisruptively and reproducibly activate astrocytes. Using a high-numerical-aperture objective, the femtosecond, pulsed laser can be focused on the cell membrane and lead to photoporation with uncertain mechanism, but accurately targeting the plasma membrane is not easily achievable and this method lacks a specific molecular target.<sup>23,29</sup> However, our technique not only confines calcium uncaging to less than femtoliter volumes,<sup>30</sup> but also enables astrocyte activation more operationally without a specific focus on plasma membrane for photostimulation.

In conclusion, calcium uncaging caused by femtosecond laser stimulation using intravital two-photon microscopy imaging offers a promising strategy to target specific regions, especially subcellular structures, in astrocytes and trigger calcium uncaging with finely controlled, high spatiotemporal resolution, and high stimulation accuracy *in vivo*. Coupling with the nonlinear excitation of a long-wavelength IR pulse laser and high-numerical-aperture objective, this strategy can reduce or even avoid out-of-focus photobleaching and photodamage while improving depth penetration for photostimulation *in vivo*. Owing to its high peak intensity and low pulse power, the femtosecond laser seldom damages the cells while offering high

efficiency and precision.<sup>31,32</sup> Therefore, the reported optical technique of astrocyte activation has the potential to facilitate physiological dynamics of astrogenesis-related vasodilation in deep brain regions *in vivo* and improve CBF in order to prevent brain ischemia, subsequently leading to the restoration of neurovascular function in neurodegeneration.<sup>33</sup>

### Acknowledgments

This research is supported by TT and WF Chao Foundation and John S Dunn Research Foundation to S.T.C.W. Y.C. is partially supported by Nantz National Alzheimer Center at Houston Methodist Hospital.

### References

1. Y. Wen et al., "Transient cerebral ischemia induces site-specific hyperphosphorylation of tau protein," *Brain Res.* **1022**(1–2), 30–38 (2004).
2. E. Farkas and P. G. Luiten, "Cerebral microvascular pathology in aging and Alzheimer's disease," *Prog. Neurobiol.* **64**(6), 575–611 (2001).
3. C. Iadecola, "Neurovascular regulation in the normal brain and in Alzheimer's disease," *Nat. Rev. Neurosci.* **5**(5), 347–360 (2004).
4. R. Deane et al., "RAGE mediates amyloid-beta peptide transport across the blood-brain barrier and accumulation in brain," *Nat. Med.* **9**(7), 907–913 (2003).
5. J. C. de la Torre, "Alzheimer disease as a vascular disorder—nosological evidence," *Stroke* **33**(4), 1152–1162 (2002).
6. Y. He et al., "Regional coherence changes in the early stages of Alzheimer's disease: a combined structural and resting-state functional MRI study," *Neuroimage* **35**(2), 488–500 (2007).
7. A. W. Kraft et al., "Attenuating astrocyte activation accelerates plaque pathogenesis in APP/PS1 mice," *FASEB J.* **27**(1), 187–198 (2013).
8. J. L. Stobart and C. M. Anderson, "Multifunctional role of astrocytes as gatekeepers of neuronal energy supply," *Front Cell Neurosci.* **7**, 38 (2013).
9. B. V. Zlokovic, "Neurovascular mechanisms of Alzheimer's neurodegeneration," *Trends Neurosci.* **28**(4), 202–208 (2005).
10. R. Deane et al., "Clearance of amyloid-beta peptide across the blood-brain barrier: implication for therapies in Alzheimer's disease," *CNS Neurol. Disord. Drug Targets* **8**(1), 16–30 (2009).
11. B. Ransom, T. Behar, and M. Nedergaard, "New roles for astrocytes (stars at last)," *Trends Neurosci.* **26**(10), 520–522 (2003).
12. M. Zonta et al., "Neuron-to-astrocyte signaling is central to the dynamic control of brain microcirculation," *Nat. Neurosci.* **6**(1), 43–50 (2003).
13. T. Takano et al., "Astrocyte-mediated control of cerebral blood flow," *Nat. Neurosci.* **9**(2), 260–267 (2006).
14. X. Wang et al., "Astrocytic Ca<sup>2+</sup> signaling evoked by sensory stimulation in vivo," *Nat. Neurosci.* **9**(6), 816–823 (2006).
15. V. Kalchenko et al., "In vivo characterization of tumor and tumor vascular network using multi-modal imaging approach," *J. Biophotonics* **4**(9), 645–649 (2011).
16. J. D. Driscoll et al., "Two-photon imaging of blood flow in the rat cortex," *Cold Spring Harb. Protoc.* **2013**(8), 759–767 (2013).
17. E. B. Brown et al., "Photolysis of caged calcium in femtoliter volumes using two-photon excitation," *Biophys. J.* **76**(1), 489–499 (1999).
18. T. Sasaki et al., "Application of an optogenetic byway for perturbing neuronal activity via glial photostimulation," *Proc. Natl. Acad. Sci. U. S. A.* **109**(50), 20720–20725 (2012).
19. V. Vedam-Mai et al., "Deep brain stimulation and the role of astrocytes," *Mol. Psychiatry* **17**(2), 124–131 (2012).
20. C. Stosiek et al., "In vivo two-photon calcium imaging of neuronal networks," *Proc. Natl. Acad. Sci. U. S. A.* **100**(12), 7319–7324 (2003).
21. J. Schummers, H. B. Yu, and M. Sur, "Tuned responses of astrocytes and their influence on hemodynamic signals in the visual cortex," *Science* **320**(5883), 1638–1643 (2008).
22. A. F. McCaslin et al., "In vivo 3D morphology of astrocyte-vasculature interactions in the somatosensory cortex: implications for neurovascular coupling," *J. Cereb. Blood Flow Metab.* **31**(3), 795–806 (2011).
23. Y. Zhao et al., "Photostimulation of astrocytes with femtosecond laser pulses," *Opt. Express* **17**(3), 1291–1298 (2009).
24. M. Cortes-Canteli et al., "Fibrinogen and beta-amyloid association alters thrombosis and fibrinolysis: a possible contributing factor to Alzheimer's disease," *Neuron* **66**(5), 695–709 (2010).
25. T. O'Connor et al., "Phosphorylation of the translation initiation factor eIF2 $\alpha$  increases BACE1 levels and promotes amyloidogenesis," *Neuron* **60**(6), 988–1009 (2008).
26. N. J. Maragakis and J. D. Rothstein, "Mechanisms of disease: astrocytes in neurodegenerative disease," *Nat. Clin. Pract. Neurol.* **2**(12), 679–689 (2006).
27. R. Dermietzel et al., "Gap-junctions between cultured astrocytes—immunocytochemical, molecular, and electrophysiological analysis," *J. Neurosci.* **11**(5), 1421–1432 (1991).
28. M. V. L. Bennett et al., "New roles for astrocytes: gap junction hemichannels have something to communicate," *Trends Neurosci.* **26**(11), 610–617 (2003).
29. M. Choi et al., "Label-free optical activation of astrocyte in vivo," *J. Biomed. Opt.* **16**(7), 075003 (2011).
30. W. Denk, "Two-photon scanning photochemical microscopy: mapping ligand-gated ion channel distributions," *Proc. Natl. Acad. Sci. U. S. A.* **91**(14), 6629–6633 (1994).
31. W. Watanabe et al., "In vivo manipulation of fluorescently labeled organelles in living cells by multiphoton excitation," *J. Biomed. Opt.* **13**(3), 031213 (2008).
32. U. K. Tirlapur and K. Konig, "Targeted transfection by femtosecond laser," *Nature* **418**(6895), 290–291 (2002).
33. Y. Chen et al., "In vivo optical activation of astrocytes as a potential therapeutic strategy for neurodegenerative diseases," *Proc. SPIE* **8565**, 85655K (2013).